Supporting Information

Dual-regulation charges separation tactics with synergistic effect of 1D/0D heterostructure and inserted ferroelectric layer for boosting photoelectrochemical water oxidation

Yanfang He [a], Jianfei Zhu [b], Youwen Yuan [b], Ying Yang [b], Yuan Liu [b], Mingming Chen [b], Dawei Cao [b,*], Xiaohong Yan [a,b,*]

[a] School of Material Science and Engineering, Jiangsu University, Zhenjiang 212013, P. R. China

[b] College of Physics and Electronic Engineering, Jiangsu University, Zhenjiang 212013, P. R. China

* Corresponding authors. E-mail: dwcao@ujs.edu.cn; yanxh@ujs.edu.cn

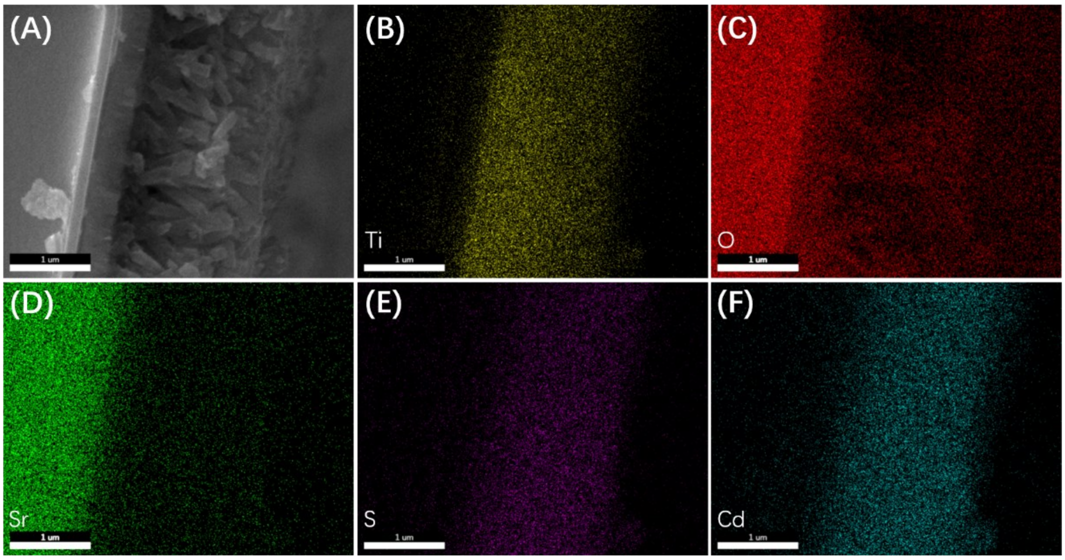

Figure S1. (A-F) EDS elemental mapping of TiO_2/STO/CdS heterostructure.

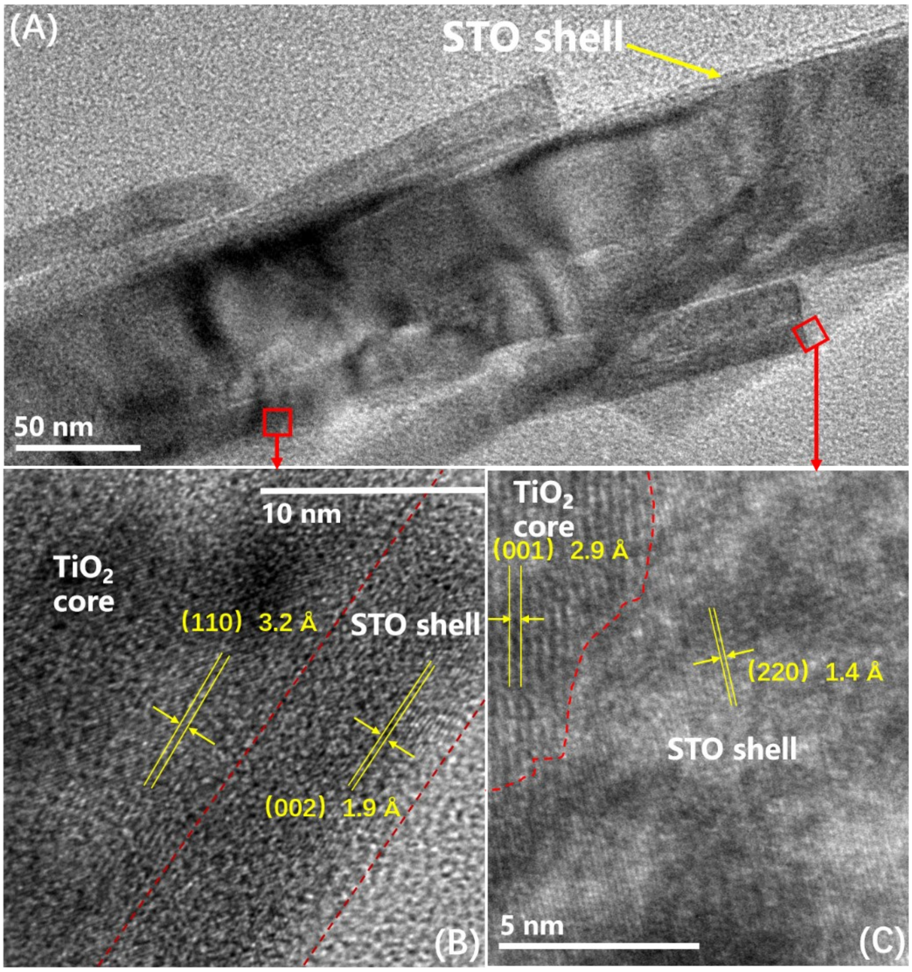

Figure S2. (A) TEM image of a TiO_2/STO heterostructure. (B) HRTEM image of TiO_2/STO for the axial surface of nanorod. (C) HRTEM image of TiO_2/STO for the top of nanorod.

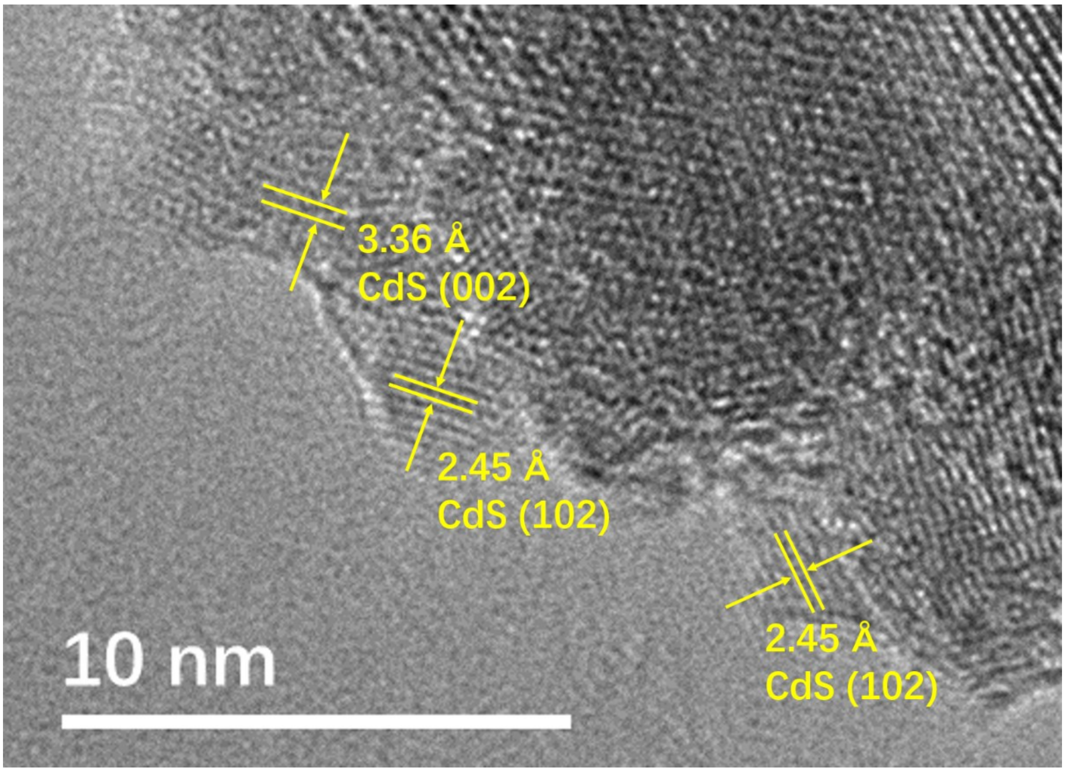

Figure S3. HRTEM image of CdS QDs on the surface of TiO_2/STO.

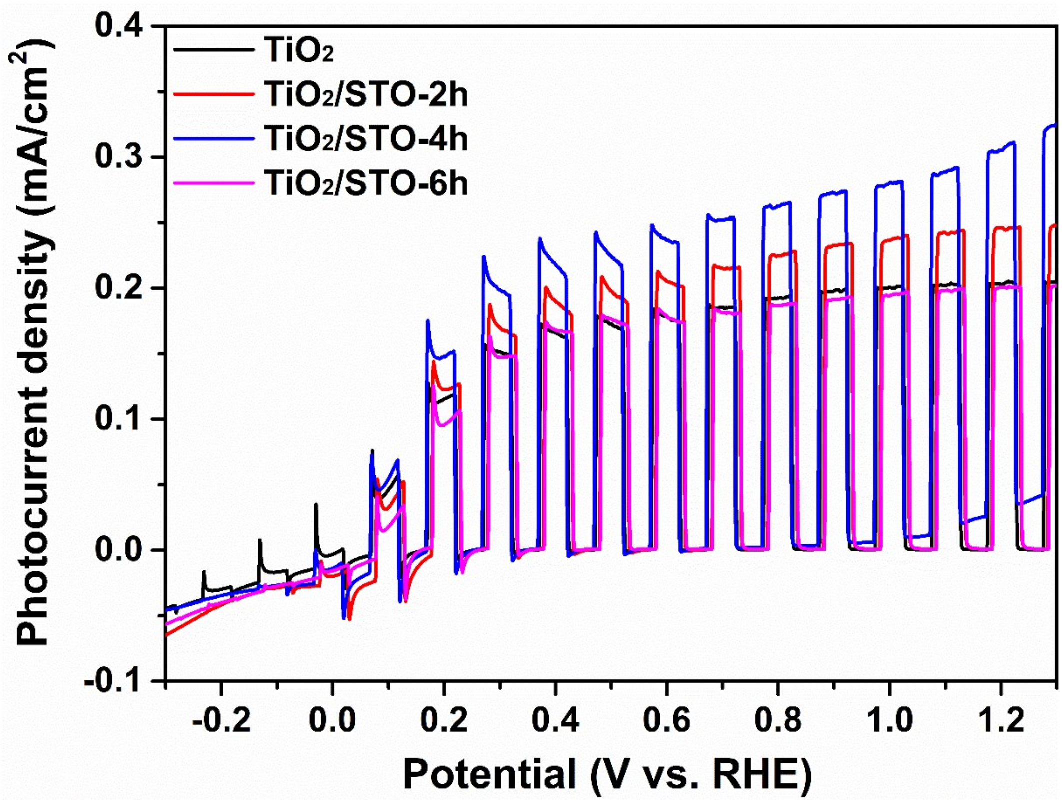

Figure S4. Chopped light photocurrent–potential curves of TiO_2, TiO_2/STO-2h, TiO_2/STO-4h and TiO_2/STO-6h, respectively.

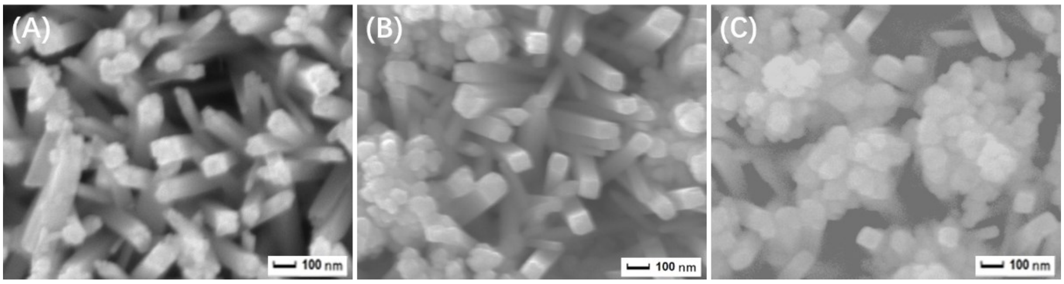

Figure S5. SEM images of (A) TiO_2/STO-2h, (B) TiO_2/STO-4h and (C) TiO_2/STO-6h.

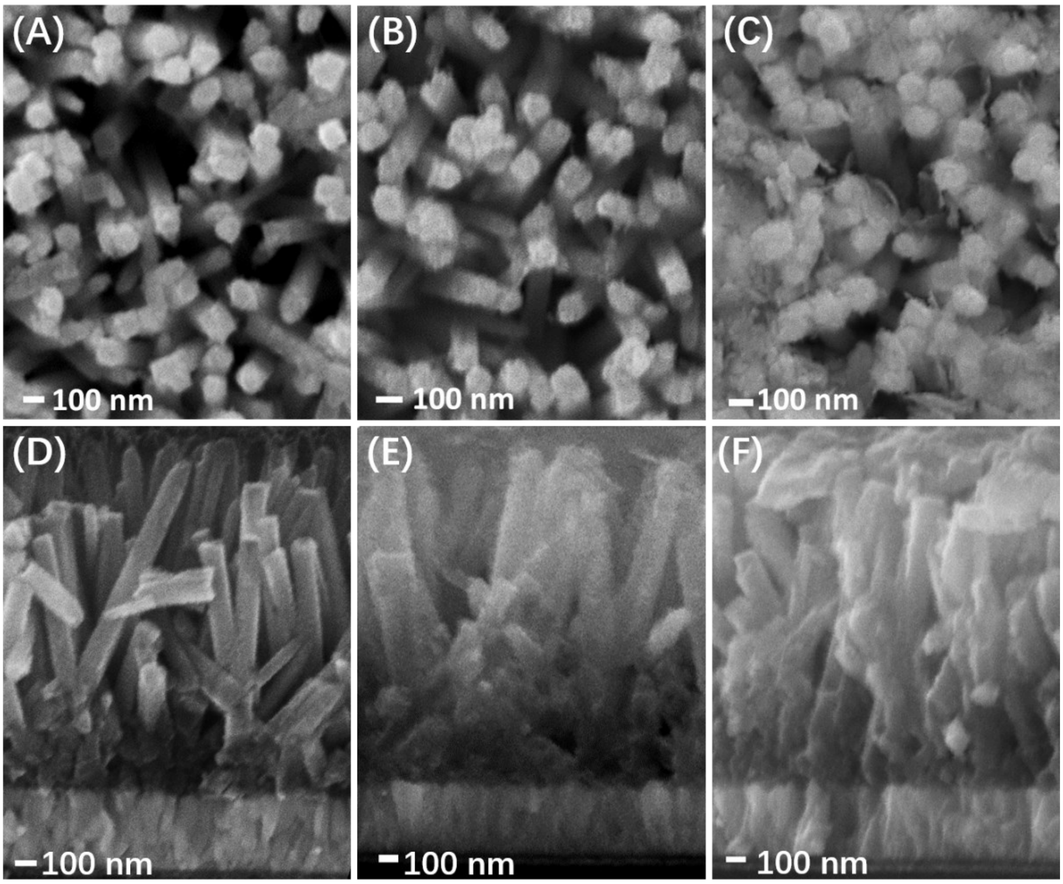

Figure S6. (A-C) SEM images of TiO_2/STO/CdS1, TiO_2/STO/CdS2 and TiO_2/STO/CdS3, respectively. (D-F) Cross-sectional SEM images of TiO_2/STO/CdS1, TiO_2/STO/CdS2 and TiO_2/STO/CdS3, respectively.

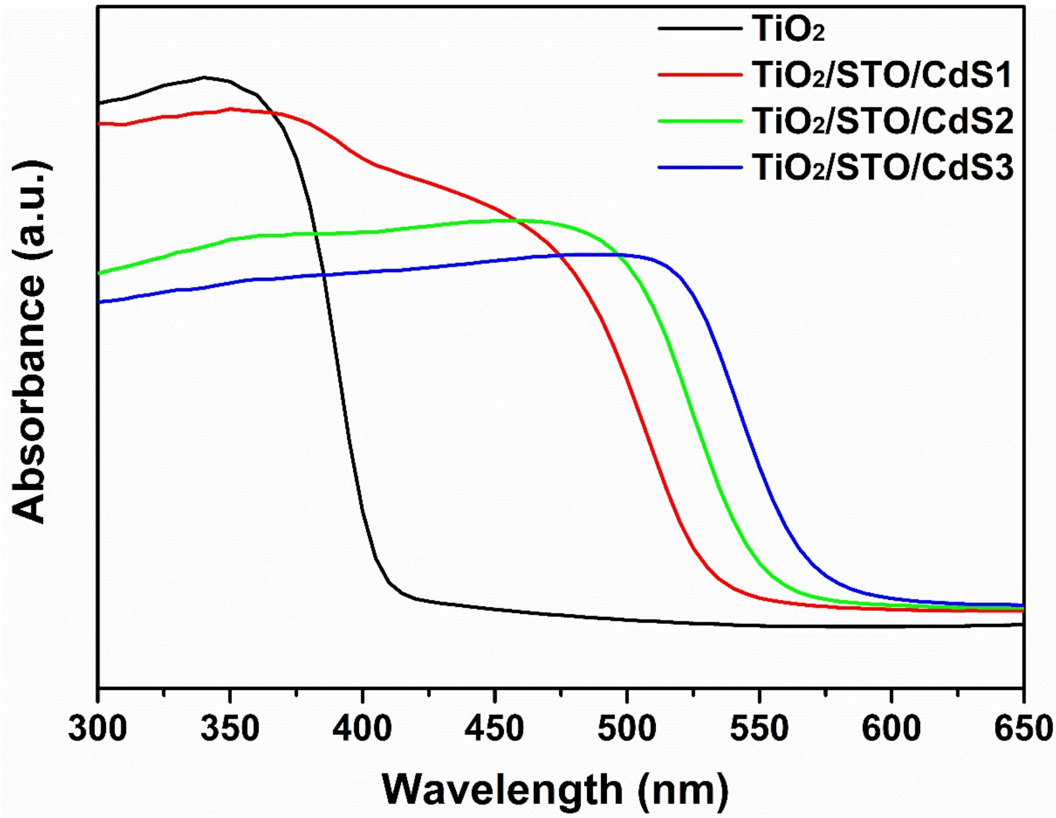

Figure S7. UV–visible DRS of the photoanodes.

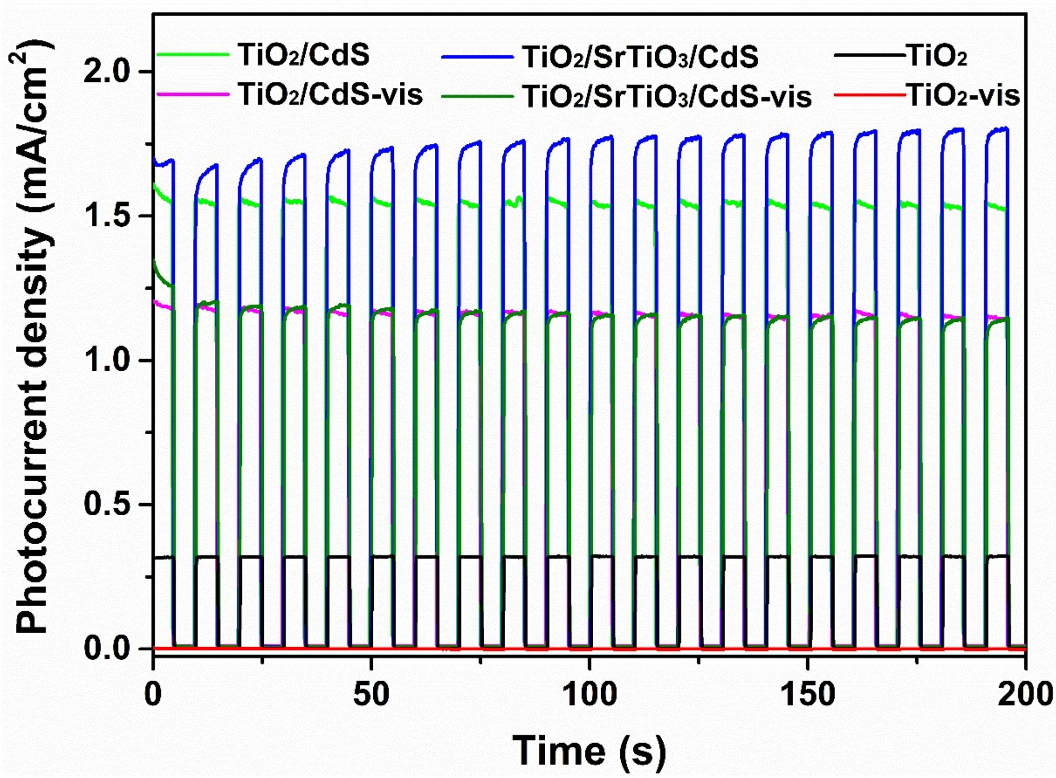

Figure S8. Photocurrent density ON–OFF curves under solar light and vis light.

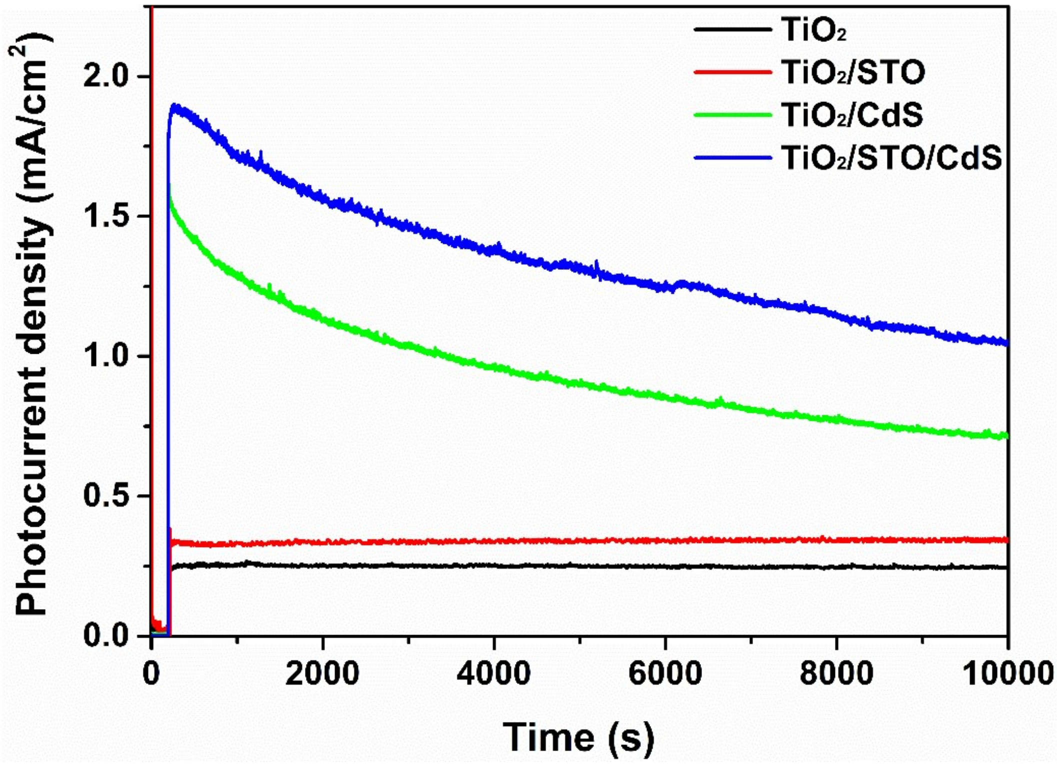

Figure S9. Photocurrent densities of TiO_2, TiO_2/STO, TiO_2/CdS and TiO_2/STO/CdS running for 10000 s.

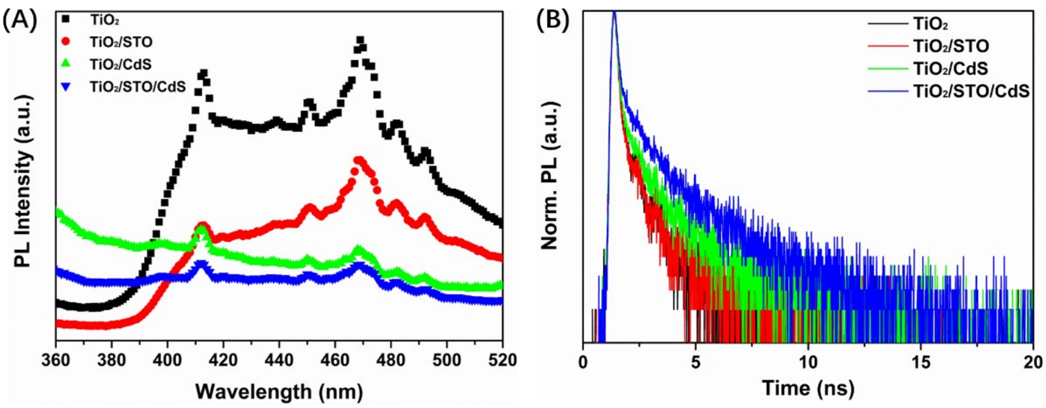

Figure S10. (A) PL and (B) Time-resolved PL spectra for TiO_2, TiO_2/STO, TiO_2/CdS and TiO_2/STO/CdS.

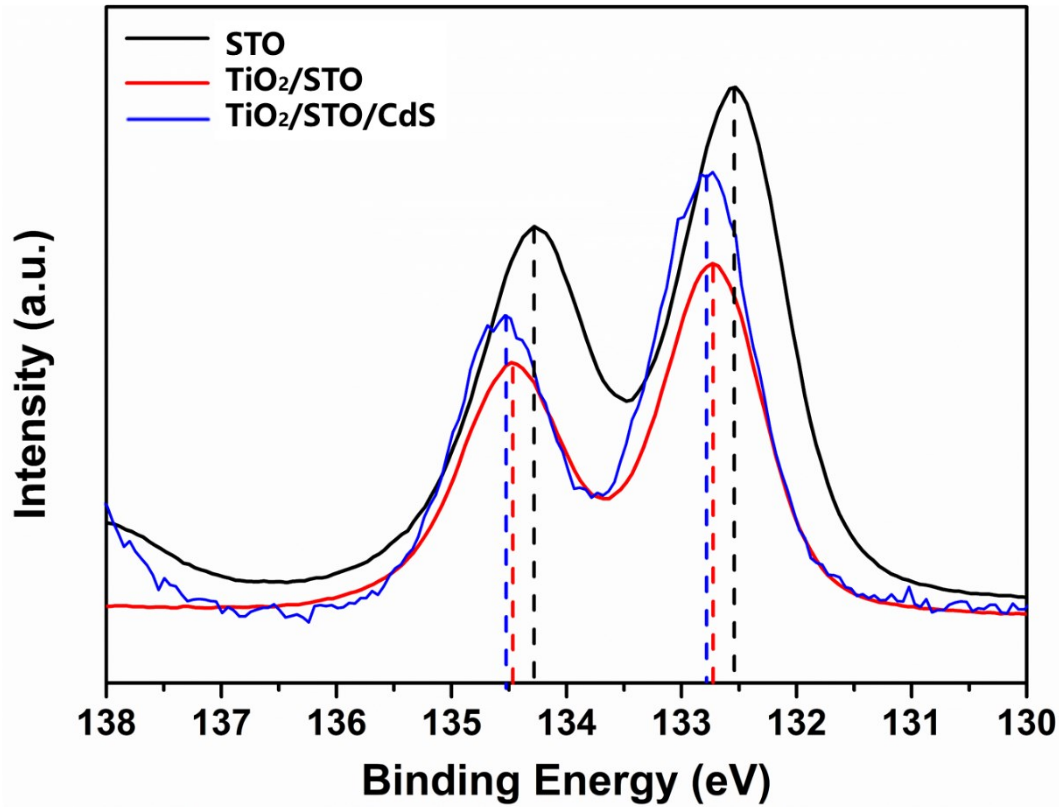

Figure S11. High-resolution XPS spectra of Sr 3d from STO, TiO_2/STO and TiO_2/STO/CdS NRs.

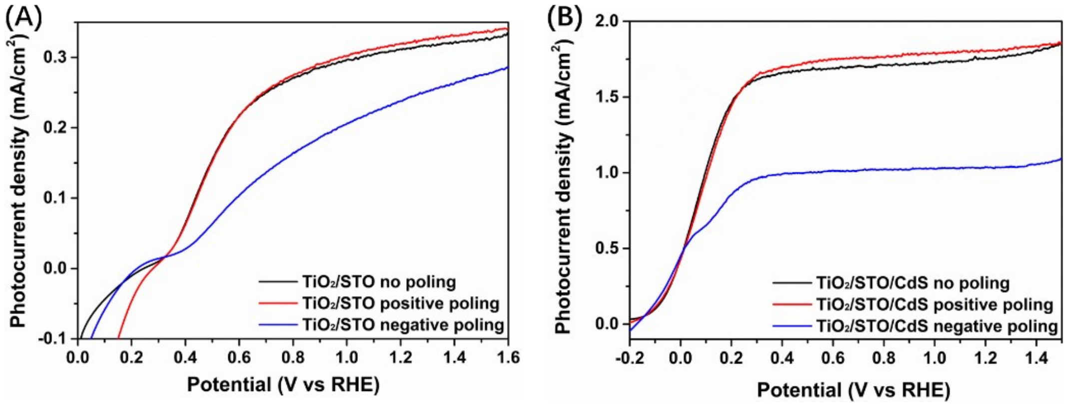

Figure S12. LSV curves of (A) TiO_2/STO and (B) TiO_2/STO/CdS with no poling, positive poling and negative poling.

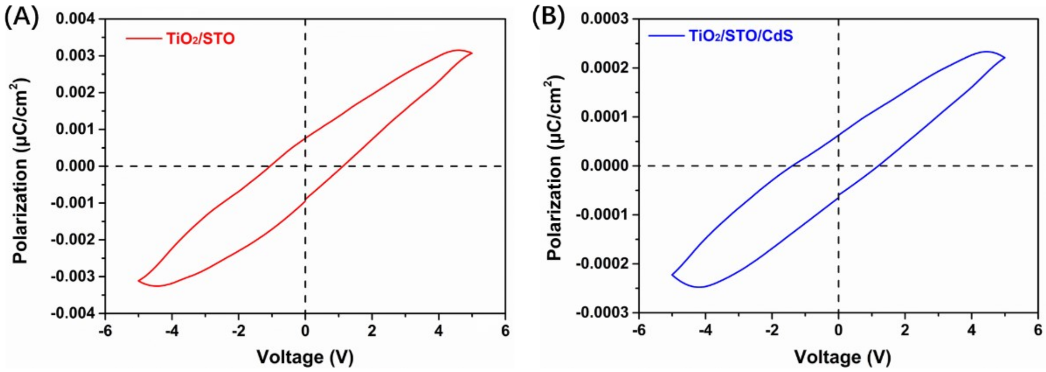

Figure S13. Polarization-electric field hysteresis loops measured from (A) TiO_2/STO and (B) TiO_2/STO/CdS NRs.

Kelvin probe force microscopy (KPFM) measures the contact potential different (CPD) between the probe and sample surface, which can further be related to the surface charging.[1] Accordingly, we implement KPFM measurement to investigate the polarized charges on STO. Figure R8 shows KPFM images of single TiO_2/STO nanorod on ITO substrate. The topography of the surface for the TiO_2/STO nanorod is presented in Figure R8A (nanorod-shaped bright spot in the center of the picture). The CPD distribution (Figure R8B) correlates with the topography observed in Figure R8A. Figure R8C shows the line profiles of the surface potential along the red line on Figure R8B, a positive surface potential difference of 15 mV is obtained on the surface of the TiO_2/STO nanorod, which confirms the existence of induced surface positive charge.[2]

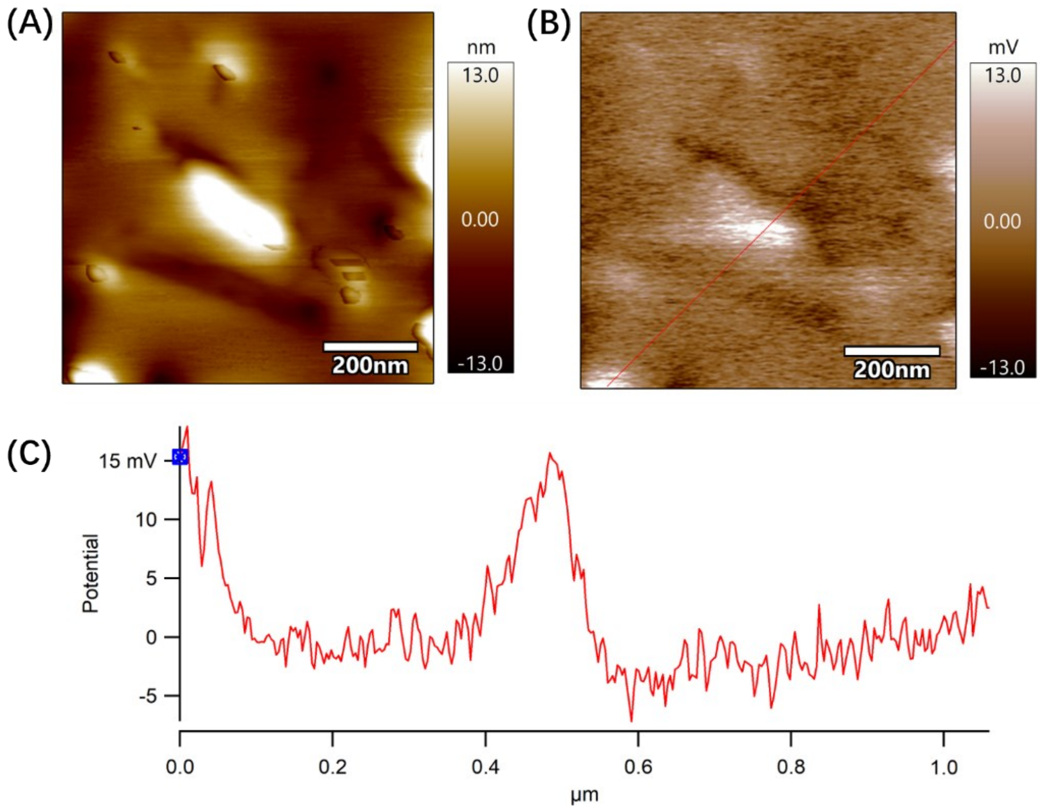

Figure S14. (A) KPFM topography and (B) surface potential maps of the very same area for single TiO_2/STO nanorod on ITO substrate. (C) CPD distribution along the red line on (B).

References

1. L. Collins, R. K. Vasudevan and A. Sehirlioglu, *ACS Applied Materials & Interfaces*, 2020, **12**, 33361-33369.
2. J. Y. Son, S. H. Bang and J. H. Cho, *Applied Physics Letters*, 2003, **82**, 3505-3507.